Available online at www.sciencedirect.com
SCIENCE DIRECT
Journal of Organometallic Chemistry 691 (2006) 2701–2707
Journal of Organometallic Chemistry
www.elsevier.com/locate/jorganchem

Synthesis and characteristics of bis(2,4-dimethyl-8-quinolinolato)-(triphenylsilanolato)aluminum (III): A potential hole-blocking material for the organic light-emitting diodes

J.T. Lim [a], C.H. Jeong [a], J.H. Lee [a], G.Y. Yeom [a,*], H.K. Jeong [b], S.Y. Chai [b], I.M. Lee [b], W.I. Lee [b]

[a] *Department of Materials Science and Engineering, SungKyunKwan University, 300 Chun-Chun-Dong, Suwon, Kyung-Gi-Do 440-746, Republic of Korea*
[b] *Department of Chemistry, Inha University Inchon, Yonghyun-dong, Nam-ku 402-751, Republic of Korea*

Received 16 August 2005; received in revised form 31 January 2006; accepted 2 February 2006
Available online 20 March 2006

Abstract

A new five-coordinated bis(2,4-dimethyl-8-quinolinolato)(triphenylsilanolato)aluminum (III) (24MeSAlq) material, having bulky substituents, was prepared in one-step reaction and was characterized. The photoluminescent (PL) spectrum of 24MeSAlq shows the largest hypsochromic shift exhibiting the maximum wavelength at the peak of 461 nm among the blue-emitting q_2AlOR-type complexes (q = 8-quinolinolato ligand and OR = aryloxy or alkoxy ligand) reported. The deep blue device composed of ITO/2-TNATA (60 nm)/NPB (15 nm)/24MeSAlq (20 nm)/Alq_3 (45 nm)/LiF (1 nm)/Al (100 nm), which uses 24MeSAlq as a hole-blocking layer and applies a principle efficiently confining an exciton recombination zone into a hole transporting layer, shows the maximum electroluminescent (EL) at the peak of 446 nm originating from the NPB emissive layer. This is attributed to an excellent hole-blocking property due to the high HOMO (highest occupied molecular orbital) energy level (6.14 eV).

Keywords: 24MeSAlq; HBL; Hole-blocking material; 8-Hydroxy-quinoline; OLED

1. Introduction

The organic light-emitting diode (OLED) has become one of the most promising next-generation large-area flat panel displays since Tang and VanSlyke reported an efficient double layered OLED utilizing tris(8-quinolinolato-N^1,O^3) aluminum (III) (Alq_3) [1,2] and has been widely studied since the display panel fabricated by a Japanese OLED manufacturer, Pioneer, was put to the market in 1998 [3].

Since then, many aluminum complexes based on the quinoline ligands such as q_3Al (q = 8-quinolinolato ligand and Al = aluminum) [4–6], q_2AlOR (OR = aryloxy or alkoxy ligand) [5,7–9], and q_2AlOAlq_2-type complexes [10] have been developed and have been demonstrated to be useful emissive materials or/and hole-blocking/electron-transporting materials [11]. Kwong et al. [11] reported on the operating stability and the luminous efficiency of an orange-red electrophosphorescent device with a variety of hole and exciton blocking materials of the q_2AlOR-type complexes. Among these complexes, the device using bis(2-methyl-8-quinolinolato)(4-phenylphenolato)aluminum (III) (BAlq) showed the excellent hole blocking property indicating a maximum efficiency of 17.6 cd A^{-1} with a projected operational lifetime of 15,000 h normalized to 100 cd m^{-2}.

Concerning the aluminum complexes based on the quinoline ligands, several luminescent characteristics have been demonstrated [4,12–15]. The light-emission of q_3Al-type and q_2AlOR-type complexes is mostly attributed to the $\pi \rightarrow \pi^*$ transition of a quinolinolato ligand rather than a

* Corresponding author. Tel.: +82 31 299 6560; fax: +82 31 299 6565.
E-mail address: gyyeom@skku.edu (G.Y. Yeom).

0022-328X/$ - see front matter © 2006 Elsevier B.V. All rights reserved.
doi:10.1016/j.jorganchem.2006.02.002

phenolato ligand. The filled π orbital (location of the highest occupied molecular orbital or HOMO) is located on the phenoxide ring and unfilled π^* orbital (location of the lowest unoccupied molecular orbital or LUMO) on the pyridyl ring. Generally, in the case of q_3Al-type complexes, the introduction of an electron-donating substituent into the pyridyl ring raises the energy level of LUMO relatively more as compared with the energy raising of HOMO, resulting in a hypsochoromic shift (blue shift) of the emissive light. On the other hand, the introduction of the electron-donating substituent into the phenoxide ring raises the energy level of the HOMO relatively more as compared with the energy raising of LUMO, leading to a bathochromic shift of the emissive light. Also, as it decreases the covalent nature between the central atom (boron, aluminum, etc.) and nitrogen atom on the quinoline ligand, the wavelength of complexes shows a hypsochromic shift. For example, the lithium terta-(2-methyl-8-quinolinolato)boron complex, in which boron is coordinated to the ligand only through a B–O bond due to the small size of boron atom relative to aluminum atom, shows more hypsochromic-shifted emission than the electroluminescent (EL) spectrum of Alq_3 (about 530 nm), exhibiting that at 470 nm [16]. Therefore, the q_2AlOR-type complexes with the five-coordination number is expected to show an intensive hypsochromic shifts rather than the q_3Al-type complexes with the six-coordination number due to decreasing of the number of the M–N bonding between the central aluminum metal (M) and a nitrogen atom (N) on the quinolinolato ligand [5,7–9].

In this paper, in order to develop a large band-gap emissive material among the q_2AlOR-type complexes for the OLEDs, a five-coordinated 24MeSAlq molecule was designed, where two methyl groups were substituted to 2,4-position proton on the pyridyl ring of the 8-qunolinolato ligand to obtain a hypsochromic-shifted emission and where the triphenylsiloxy group was used as a bulky substituent to reduce an intermolecular interaction. The 24MeSAlq material was characterized through spectroscopic analyses, thermal behaviour, the electrochemical band gap, and so on. Also, for the application of the 24MeSAlq material as a hole-blocking layer (HBL) to OLEDs, the hole-blocking properties of 24MeSAlq was discussed through the electroluminescent spectrum and the current–voltage–luminance characteristic of the blue device utilizing 24MeSAlq as a hole-blocking material and compared with the device of the same structure using other hole-blocking material, which is fabricated by a principle confining an exciton recombination zone only into the hole-transporting layer (HTL).

2. Experimental

2.1. General

The reaction was carried out under vacuum or under a nitrogen atmosphere using either standard vacuum-manifolders or inert-atmosphere dry boxes. All solvents were freshly distilled using the appropriate drying agents under a nitrogen atmosphere and all chemicals were a reagent grade without further purification.

^{1}H and ^{13}C nuclear magnetic resonance (NMR) spectra were measured using a NMR spectrometer (400.133 MHz) with tetramethylsilane (TMS) as an internal standard (Varian Unity-400, Varian Inc.). The infrared (IR) spectrum was measured as KBr pellets on an IR spectrophotometer (IFS 66/S, BRUKER Co., Ltd.). The identification of fragment patterns and molecular ions of the synthesized material was obtained by a gas chromatography/mass spectrometry data (GC/MSD) system (Agilent 6890GC/5973N MSD, Agilent Technologies, Ltd.). The quantitative analysis of carbon, proton, and nitrogen was performed by an elemental analyser (EA) (EA-1110, CE Inst. Co., Ltd.). The photoluminescence (PL) spectrum of the films deposited on the quartz substrate and the absorption spectrum in the solution were recorded with a spectrofluorophotometer (RF-5301PC, Shimazu Co., Ltd.) and a ultraviolet–visible (UV–Vis) spectrophotometer (Lambda 40, Perkin–Elmer Inc.), respectively.

The differential scanning calorimeter (DSC) measurement and the thermogravimetric analysis (TGA) were performed using a DSC analyser (DSC6100, SEICO INST.) and a Seiko Exster6000 system with a thermogravimetic analyser (TG/DTA6100, SEICO INST.), respectively. A heating rate of 10 °C min^{-1} with a nitrogen flow of 75 ml min^{-1} was used with the temperature range from 25 to 490 °C for the DSC or to 940 °C for the TGA.

2.2. Cyclic voltammetric measurements

Experiments on the cyclic voltammetry were carried out in a three-electrode compartment cell with a total volume of electrolyte solution (0.1 M tetra(*n*-butyl)ammonium perchlorate [$(n\text{-Bu})_4NClO_4$] in acetonitrile) of 20 ml. All potential were measured against a Ag/AgCl (sat. KCl) electrode (0.197 V versus NHE) as the reference electrode, a platinum wire as a counter electrode, and an indium tin oxide (ITO) film having the effective area of 12 mm^2 as a working electrode, on which the 100 nm 24MeSAlq thin film was deposited by thermal evaporation. The measurements were performed using a potentiostat (CHI660B, CH Instruments, Ltd.) under an argon atmosphere.

2.3. Preparation of bis(2,4-dimethyl-8-quinolinolato)(triphenylsilanolato)aluminum (III) (24MeSAlq)

2,4-Dimethyl-8-hydroxyquinoline was prepared by modifying the procedure reported by Phillips et al. [17], which included the synthesis of a ketoenamine intermediate by the reaction between 2-amino-phenol and 2,4-pentandione followed by the condensation reaction to prepare 2,4-dimethyl-8-hydroxyquinoline under an acid catalyst such as sulfuric acid.

24MeSAlq was synthesized through the homogeneous-phase reaction between aluminium iso-propoxide and two ligands (2,4-dimethyl-8-quinolinol and triphenylsilanol) at the reflux condition. A three-necked flask (250 ml) containing a magnetic stir bar and fitted with a reflux condenser, a rubber septum, and a gas inlet tube was charged with the tetramer of aluminum iso-propoxide (1.00 g, 1.22 mmol) and isopropanol (100 ml) under a nitrogen atmosphere. The slurry solution was heated to about 100 °C for several minutes until the solid was dissolved. The solution of isopropanol containing 2,4-dimethyl-8-quinolinol (0.84 g, 4.88 mmol) was added to the colorless solution formed over a period of 0.5 h under the reflux condition using a cannula to have a light yellow solution followed by rapid stirring for 1 h. Another solution composed of 2,4-dimethyl-8-quinolinol (0.84 g, 4.88 mmol) and triphenylsilanol (2.70 g, 9.76 mmol) dissolved in 50 ml of isopropanol was added drop by drop to the above light yellow solution over a period of 1 h under the reflux condition using the cannula. A white solid was precipitated immediately, but the solution was stirred for an additional 1 h under the reflux condition after all reactants had been added. The white precipitates were collected by filtration, washed with 50 ml of hot isopropanol and then twice with 50 ml of hot diethylether, and finally allowed to dry under a reduced pressure to yield the white powder of 24MeSAlq (2.46 g, 78%, based on aluminum iso-propoxide).

The characterization results of the 24MeSAlq material are summarized as follows: ^{1}H NMR (400.267 MHz, $CDCl_3$) δ (ppm): 7.47 (t, 2H, 6-H in quinoline, $^3J_{6,5} = 8.1$ Hz, $^3J_{6,7} = 7.8$ Hz), 7.28–7.19 (m, 11H), 7.09–7.02 (m, 10H), 2.68 (s, 3H, Me), 2.62 (s, 3H, Me); ^{13}C NMR (400.267 MHz, $CDCl_3$). δ (ppm): 156.9, 156.7, 148.2, 139.1, 138.7, 134.9, 134.8, 128.4, 127.0, 126.7, 124.6, 112.3, 110.4, 22.8, 18.7; Thermal Anal. (°C): no T_g, T_m (245.8), T_d (461.9); GC/MSD (EI) (m/z): 645 (M^+); FT-IR (KBr pellet) (cm^{-1}): 3066, 3042, 1605, 1576, 1508, 1462, 1427, 1410, 1393, 1354, 1323, 1285, 1221, 1153, 1111, 1055, 1026, 991, 937, 862, 812, 752, 702, 554, 513, 448; Anal. Calc. for $C_{40}H_{35}O_3N_2AlSi$: C, 74.28; H, 5.45; N, 4.17. Found: C, 74.52; H, 5.90; N, 4.09%.

2.4. Fabrication of the blue OLEDs

Fig. 1 exhibits the schematic device configuration and molecular structures of OLEDs. The blue OLED devices with the structure of glass/ITO (120 nm, about 10 Ω/□)/2-TNATA (60 nm)/NPB (15 nm)/24MeSAlq (20 nm) or BAlq (20 nm)/Alq_3 (35 nm)/LiF (1 nm)/Al(100 nm) were fabricated by vacuum deposition, in which 24MeSAlq or BAlq was used as a HBL/an electron-transporting layer (ETL), 4,4′,4″-tris[2-naphthylphenyl-1-phenylamino]triphenylamine (2-TNATA) as a hole-injecting layer (HIL), 4,4′-bis[*N*-(1-napthyl)-*N*-phenyl-amino]-biphenyl (NPB) as a HTL, tris[8-hydroxyquinolinonato]aluminum (III) (Alq_3) as an ETL, and lithium fluoride (LiF) as an electron-injecting layer (EIL), respectively. Before loading into a deposition chamber, the ITO substrate was cleaned with detergents and deionized water, dried in an oven at the temperature of 120 °C for 2 h. The devices were fabricated by evaporating the organic layers at the rate of 0.05–0.2 nm s^{-1} onto the ITO substrate sequentially at a pressure below 1×10^{-6} Torr. Finally, onto the EIL layer, a 100-nm-thick aluminum metal was deposited at the rate

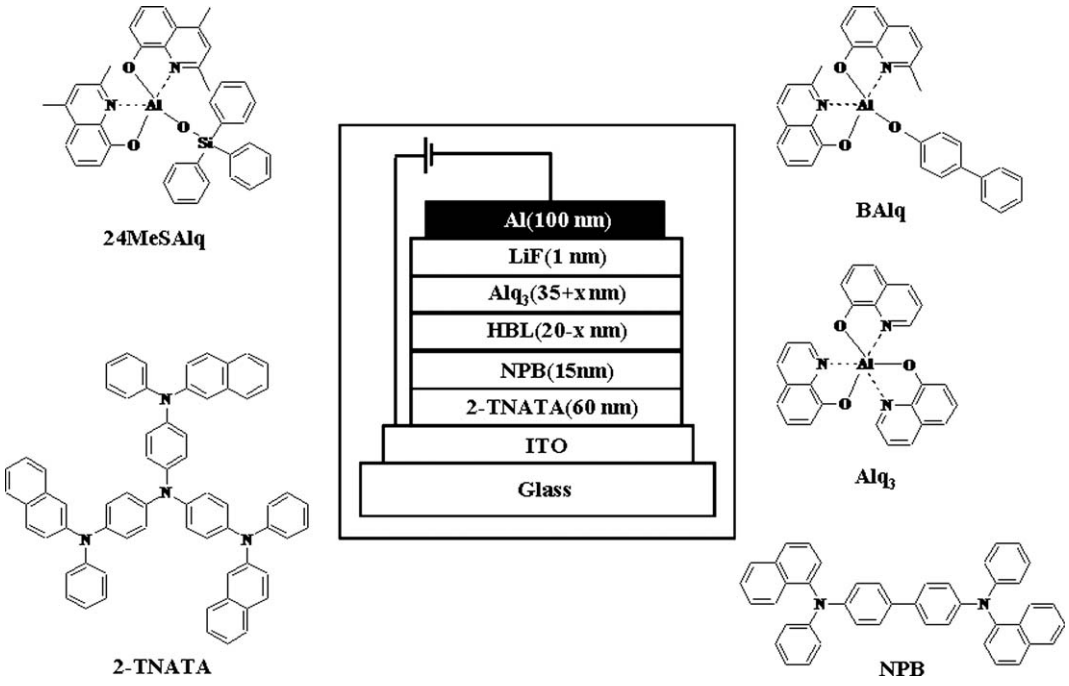

Fig. 1. Schematic configuration of the blue devices and molecular structures.

of 0.1–2 nm s^{-1} as a cathode. The emissive active area of all devices was 2 mm × 2 mm.

2.5. Photometric properties of the blue OLEDs

Current–voltage characteristics were measured with a source-measure unit (236, Keithley Instrument Inc.). The intensities from the blue emission of the devices were measured by the photocurrent induced on the silicon photodiodes using a picoammeter (485, Keithley Instruments Inc.). The EL spectra of the as-fabricated blue devices were measured by optical emission spectroscopy (PCM-420, SC Tech. Inc.).

3. Results and discussion

3.1. Thermal stability of 24MeSAlq

Thermal properties of 24MeSAlq were evaluated by simultaneous thermal analysis, where TGA and DSC experiments were run simultaneously; therefore, thermal events observed in the DSC could be directly correlated with weight loss events.

The morphological stability of Alq_3, desirable for the practical OLED applications, has been attributed to its intrinsic polymorphic, a racemic nature, and strong dipolar interactions. Several phase transitions were observed for Alq_3 and these phase transitions affecting the optical properties of the OLED device are attributed to polymorphism of the crystalline material as discussed by Brinkmann et al. [18], assigning an exothermic phase transition from α-Alq_3 to γ-Alq_3 phase at about 395 °C, as it was confirmed by X-ray diffraction. In the case of 24MeSAlq, as shown in the inset of Fig. 2 for the DSC curve of 24MeSAlq measured at the heating rate of 10 °C min^{-1}, no phase transition and no glass transition was observed prior to T_m, while it shows a sharp melting point at 246 °C. In addition, when the remelting stability was tested using ^1H NMR and FT-IR with the material left in the melting tube just past the major endothermic transition (T_m), no decomposition product could be observed by the analyses. Also, the 24MeSAlq material exhibited an onset of the endothermic decomposition at about 340 °C and showed the largest one at 462 °C as shown in the DSC curve. Meanwhile, as shown in Fig. 2 for the TGA curve of 24MeSAlq, the maximum rate of weight loss of 24MeSAlq took place at 420 °C and the weight loss of 5% and 10% were occurred at 329 and 349 °C, respectively. In results, the temperature range to deposit the thermally stable 24MeSAlq thin film by thermal evaporation is expected to be from 246 °C (melting point) to about 340 °C (the temperature just below the start of decomposition).

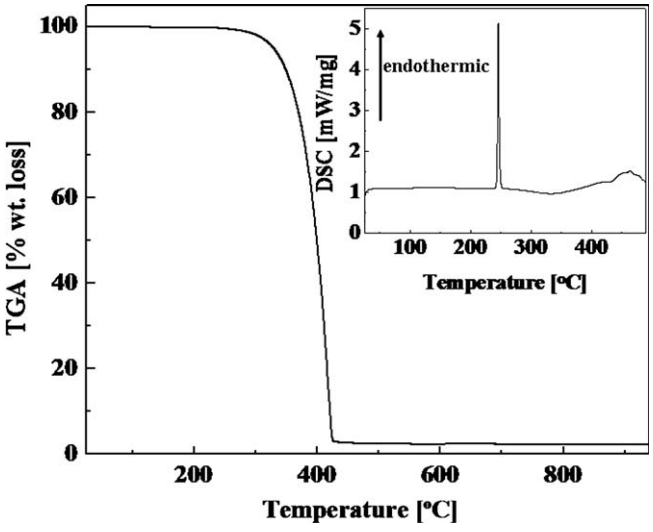

Fig. 2. TGA trace of the as-synthesized 24MeSAlq material. Inset: DSC trace of the same material. Data were measured with the heating rate of 10 °C min^{-1} in flowing nitrogen at 75 ml min^{-1}.

3.2. Optical properties of 24MeSAlq

Fig. 3 shows the PL and photoluminescence excitation (PLE) spectra of the 24MeSAlq film deposited on the quartz substrate by thermal evaporation.

The effect of the ligand in q_2AlOR-type complexes was discussed by Wang et al. [13]. As bulkiness of OR in q_2AlOR is increased, the maximum intensity in PL spectra were hypsochromic shifted because an intermolecular interaction among molecules is decreased [12]. The triphenylsilanolato ligand as a bulky ligand was introduced to reduce an intermolecular interaction. In result, as bulkiness of OR is increased, we are expected to be hypsochromic shifted in PL spectrum, due to a reduction of an electrostatic binding force among molecules.

Meanwhile, the optical transition responsible for the PL of 24MeSAlq is due to a $\pi \rightarrow \pi^*$ charge transfer from the electron rich phenoxide ring (HOMO) to the electron deficient pyridyl ring (LUMO) [13]. The energy band gap is increased with increasing the number of the methyl

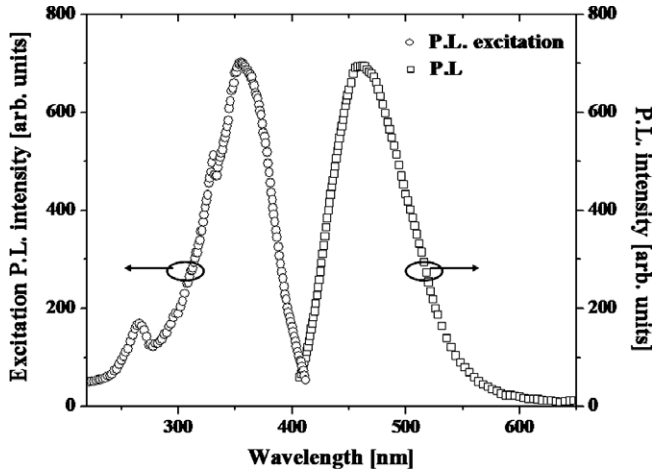

Fig. 3. PL spectrum and PLE spectrum of the 24MeSAlq thin film with the thickness of 100 nm on the quartz substrate.

substituent on the pyridyl ring in the 8-quinolinolato ligand. The PL spectrum of 24MeSAlq (λ_{max}: 461 nm) which contains the 2,4-dimethyl-8-quinolinolato ligand substituting two methyl groups on the pyridyl ring showed the hypsochromic shift of 14 nm, relative to SAlq (λ_{max}: 475 nm) [19] which has the 2-methyl-8-quinolinolato ligand substituting one methyl group on the pyridyl ring. Also, the PL spectrum of 24MeSAlq exhibited the narrow wavelength with a full-width at half-maximum (FWHM) of 81 nm when the spectrum was obtained by the excitation with the pumping wavelength of 355 nm. In the case of the PLE spectrum of 24MeSAlq, as shown in Fig. 3, two peaks at 266 and 355 nm were shown together with a shoulder peak around 331 nm.

3.3. Electrochemical properties of 24MeSAlq

In order to investigate the optical band gap, the UV–Vis absorption spectrum of the as-synthesized 24MeSAlq material in a dilute solution of chloroform (10^{-4} M) was measured and the result is shown in the inset of Fig. 4. The band gap can be estimated from a plot of $(\alpha h\nu)^2$ versus the photon energy ($h\nu$) [20]. The intercept of the tangent to the plot will give a good approximation of the band gap energy as shown in the inset of Fig. 4. The optical band gaps ($\pi \rightarrow \pi^*$) of 24MeSAlq and BAlq (not shown) complexes estimated by the intercept (or UV absorption onset) were about 3.2 and 2.97 eV, respectively.

The cyclic voltammogram of 24MeSAlq is shown in Fig. 4 and the data obtained from the cyclic voltammograms of 24MeSAlq and BAlq are summarized in Table 1. All these hole-blocking materials were deposited by thermal evaporation onto the ITO glass substrate and separately scanned both positively and negatively with a

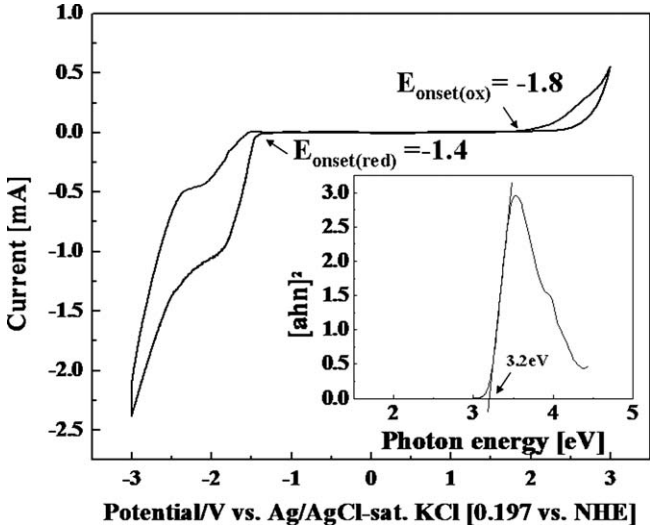

Fig. 4. Cyclic voltammogram of the 24MeSAlq film deposited onto the ITO glass in a 0.10 M $(n\text{-Bu})_4NClO_4$ solution dissolved in anhydrous acetonitrile at a scanning rate of 50 mV s^{-1}. The counter electrode was a platinum wire. Inset: plot of $(\alpha h\nu)^2$ vs. photon energy ($h\nu$) for the 24MeSAlq thin film.

Table 1
Electrochemical properties and energy levels of 24MeSAlq and BAlq as the hole blocking materials

Hole-blocking materials	$E_{onset(ox)}$ vs. Ag/AgCl (V)	$E_{onset(red)}$ vs. Ag/AgCl (V)	E^{HOMO} (eV)	E^{LUMO} (eV)	E_g^{CHEM} (eV)
24MeSAlq	1.80	−1.40	6.14	2.94	3.20
BAlq	1.54	−1.43	5.88	2.91	2.97

0.1 M $n\text{-BuN}_4ClO_4$ solution dissolved in anhydrous acetonitrile at the scanning rate of 50 mV s^{-1}. During the sweeping of the materials from the positive to negative bias, the color of the films was not changed and was remained colorless. The anodic scans of two complexes, corresponding to p-doping, show well-defined irreversible peaks. The oxidation onset potentials (versus Ag/AgCl-saturated) of 24MeSAlq and BAlq (not shown) were 1.8 and 1.54 V, respectively, and the reduction onset potentials (versus Ag/AgCl-saturated) were found to be −1.4 and −1.43 V, respectively, as shown in Fig. 4 for 24MeSAlq.

From these onset potentials of the oxidation and the reduction of cyclic votammograms, the energy levels (E^{HOMO} and E^{LUMO}) and an electrochemical band gap (E_g^{CHEM}) could be calculated. With an empirical relation obtained through the conversion of the experimental data using the valence effective Hamiltonian technique, E^{HOMO}, E^{LUMO} and E_g^{CHEM} of each complexes were calculated [21,22]. The E_g^{CHEM} values of 24MeSAlq and BAlq were calculated to be 3.20 and 2.97 eV, respectively. These E_g^{CHEM} values agree with the aforementioned optical band gap of UV–Vis spectrum. However, when the energy levels of the 24MeSAlq material with two methyl groups were compared with those of the BAlq one with one methyl group, the HOMO energy level (6.14 eV) of 24MeSAlq was higher than that (5.88 eV) of BAlq material but the LUMO energy values of 24MeSAlq (2.94 eV) and BAlq (2.91 eV) materials were similar each other. The obtained results are different from the results obtained by Sugimoto and Sakaki [14], possibly due to the different material characteristics between the q_3Al-type complexes and q_2AlOR-type complexes, where the LUMO energy level was raised relatively higher than the HOMO energy level in the q_3Al-type complexes as the number of the methyl group on the pyridyl ring were increased. The higher HOMO level of 24MeSAlq than that of BAlq obtained in the experiment is expected to confine a hole/exciton effectively inside the emissive layer of HTL due to the better hole-blocking property. The electron-transporting ability of two materials is also expected to have a similar trend.

3.4. Optical properties of the blue OLEDs

The inset of Fig. 1 shows a schematic configuration of the blue OLED which is composed of glass/ITO (120 nm)/2-TNATA (60 nm)/NPB (15 nm)/HBL (20 nm)/Alq_3 (35 nm)/LiF (1 nm)/Al (100 nm) (HBL: 24MeSAlq (device A) or BAlq (device B)). Meanwhile, the green

OLED of device C is composed of glass/ITO (120 nm)/2-TNATA (60 nm)/NPB (15 nm)/Alq_3 (55 nm)/LiF (1 nm)/Al (100 nm). The BAlq material of device B is commonly used as a hole-blocking layer in an organic light-emitting diode [11].

The luminescence of OLEDs arises from radiative recombination of an electron and a hole. In the case of device A and device B, the fabricated blue-emitting devices yield a singlet exciton in the interfacial region of a hole-transporting layer (NPB) between NPB and 24MeSAlq. In general, by lowering the charge carrier injection barrier and in turn increasing the hole and electron injection efficiency, a better balance of opposite carrier concentration in an emissive layer can be achieved resulting in increased electroluminescent efficiency. Insertion of carrier injection assisted layers (e.g., HIL, HTL, EIL, and ETL) at both anode and cathode sides are one of such interfacial modification techniques. Consider a carrier injection in device A of Fig. 1, it is expected to process by the following the proposed hopping mechanism. Just starting from ITO (work function: about 4.7 eV) [23] as anode, a hole is injected by a hopping through 2-TNATA (E^{HOMO}: 5.1 eV) [24] as a hole-injecting layer into NPB (E^{HOMO}: 5.4 eV) [23] as a hole-transporting layer. An electron, just starting from Al (work function: 4.3 eV) [23] as cathode, is injected by a hopping through LiF (work function: 2.6 eV) [25] as an electron-injecting layer, Alq_3 (E^{LUMO}: 3.1 eV) [23] as the electron-transporting layer and 24MeSAlq (E^{LUMO} in Fig. 4: 2.9 eV) as both an electron-transporting layer and a hole-blocking layer into a NPB layer. In the case of the green-emitting device C, an exciton recombination zone can be formed broadly in the Alq_3 layer having functions as EML and ETL.

In addition, in blue devices fabricated by using a hole-blocking layer, the exciton recombination efficiency by hopping of a hole and an electron is expected to depend on a difference of HOMO energy level (ΔH) between NPB and HBL, which would confine most of a hole carrier concentration only into a NPB layer. The device A is expected to be more hypsochromic shifted in EL spectra than device B because 24MeSAlq (ΔH: 0.74 eV) have lager hole-blocking property than BAlq (ΔH: 0.48 eV).

Fig. 5 shows the EL spectra of the device A, B, and C, respectively. Comparing with device C containing the Alq_3 emitter having the maximum EL peak (EL_{max}) at 543 nm, the device A with 24MeSAlq and device B with BAlq as a hole-blocking layer exhibit EL_{max} peaks at 446 and 503 nm, respectively. Also, the EL spectra of device A, B, and C exhibit the FWHM of 65, 122, and 117 nm, respectively. As the number of methyl substituent on the pyridyl ring of the quinoline ligand is increased, the hole-blocking properties of the q_2AlOR-type complexes are improved in the blue device leading to the emissive zone in the NPB layer. As expected in device A with 24MeSAlq, bearing two methyl substituents on the pyridyl ring of the quinoline ligand, the exciton recombination zone was nearly restricted into the neighbouring NPB layer by a high

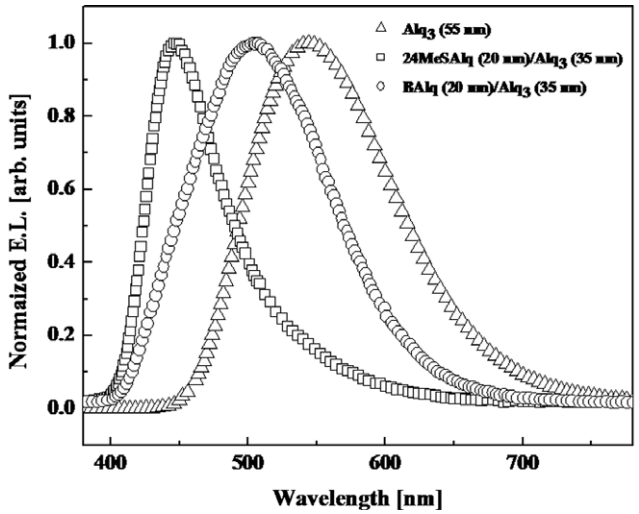

Fig. 5. EL spectra of glass/ITO/2-TNATA (60 nm)/NPB (15 nm)/HBL (20-x nm)/Alq_3 (35 + x nm)/LiF (1 nm)/Al (100 nm) (□: $x = 0$, 24MeSAlq (20 nm)/Alq_3 (35 nm); ○: $x = 0$, or BAlq (20 nm)/Alq_3 (35 nm); △: $x = 20$, Alq_3 (55 nm)).

ΔH, completely showing a real blue emission with the 65-nm-FWHM wavelength.

Meanwhile, an exciton recombination cannot be formed in the HIL of 2-TNATA (PL_{max}: 480 nm) [24] and the HBL of 24MeSAlq (PL_{max}: 461 nm). In general, the EL spectrum cannot be moved to the hypsochromic-shifted wavelength than the PL spectrum in OLEDs for itself. Meanwhile, the device B with BAlq as the HBL containing one methyl

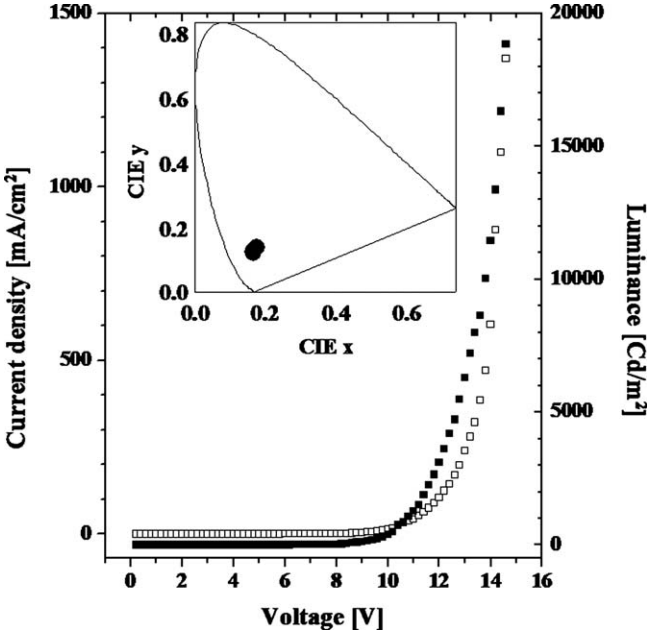

Fig. 6. Current density–voltage–luminance characteristics of the blue OLED devices composed of ITO/2-TNATA (60 nm)/NPB (15 nm)/24MeSAlq (20 nm)/Alq_3 (35 nm)/LiF (1 nm)/Al (100 nm). The inset shows the corresponding CIE chromaticity diagram with the coordinates of the spectra for the same device as a function of the voltage.

substituent on the quinolinolato ligand is mostly emitted a broad bluish-green color with 122-nm-FWHM as a result of a poor hole-blocking property.

Fig. 6 shows the current density–voltage–luminance characteristic of the deep blue OLED device (device A) with 20-nm-thick 24MeSAlq tuned by confining the recombination zone into a neighbouring HTL. The onset voltage of 20-nm-thick 24MeSAlq is 3.2 V and the external quantum efficiency and the power efficiency are about 0.82% and 0.58 lm W^{-1} at the luminance of 100 cd m^{-2} (bias voltage of 7.4 V and current density of 3.32 mA cm^{-2}). The maximum luminance is about 18,850 cd m^{-2} at 14.6 V and 1.37 A cm^{-2}. The inset of Fig. 6 shows the change of the corresponding the CIE (Commission Internationale de L'Eclairege) chromaticity coordinates for the device A when the forward bias is changed from 9 V (about 30 cd m^{-2}) to 11 V (about 1300 cd m^{-2}). As shown in the figure, the change of the forward bias from 9 to 11 V did not change the CIE chromaticity coordinates significantly, therefore, remaining in the deep blue range of 0.164–0.168, 0.127–0.135.

4. Conclusions

The 24MeSAlq was synthesized as a potential HBL material that can efficiently confine the recombination zone into HTL by one-step reaction. This new five-coordinated aluminum complex showed no glass temperature and no phase transition before the melting point. Using the 24MeSAlq material, the thermally stable thin film could be easily formed by thermal evaporation. Also, the PL spectrum of the 24MeSAlq complex shows the largest hypsochromic shift among the blue-emitting q_2AlOR-type complexes reported in the references, exhibiting the maximum PL peak of 459 nm and the HWHM of 81 nm. The blue device with the ITO/2-TNATA (60 nm)/NPB (15 nm)/24MeSAlq (20 nm)/Alq_3 (45 nm)/LiF (1 nm)/Al (100 nm) structure, efficiently forming exciton recombination into HTL, showed the maximum EL peak at 446 nm. However, in the device of the same structure using BAlq as the HBL, the EL spectrum exhibited the broad wavelength of a bluish-green color (FWHM: 122 nm). It was due to the more efficient blocking property of 24MeSAlq than BAlq caused by the higher HOMO energy level of the 24MeSAlq material than that of the BAlq material. The deep blue device with 20-nm-thick 24MeSAlq showed the maximum luminance of 18,850 cd m^{-2} at the bias voltage of 14.6 V and the current density of 1.37 A cm^{-2}.

Acknowledgements

This work was supported by Electronics and Telecommunications Research Institute (ETRI), by the National Research Laboratory Program (NRL) of Ministry of Science and Technology, and by the Ministry of Commerce, Industry and Energy (MOCIE).

References

[1] C.W. Tang, S.A. VanSlyke, Appl. Phys. Lett. 51 (1987) 913.
[2] J.H. Burroughes, D.D.C. Bradley, A.R. Brown, R.N. Marks, K. Mackay, R.H. Friend, P.L. Burn, A.B. Homes, Nature 347 (1990) 539.
[3] O. Prache, Displays 22 (2001) 49.
[4] L.S. Sapochak, A. Padmaperuma, N. Washton, F. Endrino, G.T. Schmett, J. Mrshall, D. Fogarty, P.E. Burrows, S.R. Forrest, J. Am. Chem. Soc. 123 (2001) 6300.
[5] H. Jang, L.-M. Lee, Y. Kim, T. Zyung, Y. Do, Synth. Met. 121 (2001) 1667.
[6] J. Kido, Y. Lizumi, Appl. Phys. Lett. 73 (1998) 2721.
[7] P.S. Bryran, F.V. Lovecchio, S.A. VanSlyke, US Patent No. 5141671, August 25, 1992.
[8] Y. Sato, T. Ogata, S. Ichinosawa, Y. Murata, Synth. Met. 91 (1997) 103.
[9] S.A. VanSlyke, N.Y. Rochester, US Patent No. 5151629, September 29, 1992.
[10] F. Papadimitrakopoulos, X.-M. Zhang, D.L. Thomsen III, K.A. Higginson, Chem. Mater. 8 (1996) 1363.
[11] R.C. Kwong, M.R. Nugent, L. Michalski, T. Ngo, K. Rajan, Y.-J. Tung, M.S. Weaver, T.X. Zhou, M. Hack, M.E. Thompson, S.R. Forrest, J.J. Brown, Appl. Phys. Lett. 81 (2002) 162.
[12] C.H. Chen, J. Shi, Coord. Chem. Rev. 171 (1998) 161.
[13] G. Wang, F. Lian, Z. Xie, G. Su, L. Wang, X. Jing, F. Wang, Synth. Met. 131 (2002) 1.
[14] M. Sugimoto, S. Sakaki, J. Appl. Phys. 90 (2001) 6092.
[15] A. Curioni, M. Boero, W. Andreoni, Chem. Phys. Lett. 294 (1998) 263.
[16] X.T. Tao, H. Suzuki, T. Wada, S. Miyata, H. Sadabe, J. Am. Chem. Soc. 121 (1999) 9447.
[17] J.P. Phillips, R.L. Blibingger, L.L. Merrit Jr., J. Am. Chem. Soc. 71 (1949) 3986.
[18] M. Brinkmann, G. Gadret, M. Muccini, C. Taliani, N. Masciocchi, A. Sironi, J. Am. Chem. Soc. 122 (2000) 5147.
[19] J.T Lim, M.J. Lee, N.H. Lee, Y.J. Ahn, C.H. Lee, D.H. Hwang, Curr. Appl. Phys. 4 (2004) 327.
[20] F. Gu, S.F. Wang, M.K. Lii, G.J. Zhou, D. Xu, D.R. Yuan, J. Appl. Chem. B 108 (2004) 8119.
[21] Z.K. Chen, H. Meng, Y.H. Lai, W. Huang, Macromolecules 32 (1999) 4351.
[22] J.L. Bredas, R. Silbey, D.S. Broudreux, R.R. Chance, J. Am. Chem. Soc. 105 (1983) 6555.
[23] M.A. Baldo, S.R. Forrest, Phys. Rev. B 62 (2000) 10958.
[24] K. Okumoto, Y. Shirota, J. Lumin. 87–89 (2000) 1171.
[25] L.S. Hung, C.W. Tang, M.G. Mason, P. Raychaudhri, J. Madathil, Appl. Phys. Lett. 78 (2001) 544.